Korean J. Chem. Eng., 33(2), 448-455 (2016)
DOI: 10.1007/s11814-015-0167-y

pISSN: 0256-1115
eISSN: 1975-7220

Flocculation and viscoelastic behavior of industrial papermaking suspensions

Mustafa S. Nasser*,†, Mohammed J. Al-Marri*, Abdelbaki Benamor*, Sagheer A. Onaizi, Majeda Khraisheh***, and Mohammed A. Saad*****

*Gas Processing Center, College of Engineering, Qatar University, P. O. Box 2713 Doha, Qatar
**School of Chemical Engineering and Advanced Materials, Newcastle University,
535 Clementi Road, Blk 35 #02-01, Singapore 599489, Singapore
***Department of Chemical Engineering, College of Engineering, Qatar University, P. O. Box 2713 Doha, Qatar
(*Received 26 May 2015 • accepted 30 July 2015*)

Abstract−The effects of the surface charge type and density C496, C492 and A130LMW polyacrylamides (PAMs) on the rheological behavior of real industrial papermaking suspensions were quantitatively related to the degree of flocculation for the same industrial papermaking suspensions. The floc sizes were larger but less dense when anionic PAM was used, and this due to the repulsive forces between the anionic PAM and colloidal particles, leading to the development of open structure flocs of less density. On the other hand, rheological measurements showed that the papermaking suspension is thixotropic with a measurable yield stress. The results showed that the magnitude of the critical stress, τ_c, complex viscosity, η^*, elastic modulus, G′, and viscous modulus, G″, depend on the number of interactions between the PAM chains and particle surface and the strength of those interactions. Cationic PAM showed higher values of η^*, G′, G″ and τ_c compared to anionic PAM. This behavior is in good agreement with Bingham yield stress, τ_B, adsorption and effective floc density results. Similar to oscillatory measurements, creep measurements also showed that the deformation was much lower for the cationic PAM based suspensions than for the anionic PAM based suspensions. Furthermore, the results revealed that increasing the cationic PAM surface charge decreases the floc size but increases the adsorption rate, elasticity and effective floc density proposing differences in the floc structures, which are not revealed clearly in the Bingham yield stress measurements.

Keywords: Papermaking Suspensions, Flocculation, Floc Size, Effective Floc Density, Rheology

INTRODUCTION

Paper is mainly made of cellulosic pulp fibers derived from natural bio-resources, including wood and non-wood lignocellulosic materials [1]. For most paper grades, fillers are the most important composition of the paper industry. Fillers are added to improve paper sheet optical quality and reduce production costs [2,3]. Mainly, the fillers dosages used are in the range from 3 to 30% and can even reach 38% for certain required papers [4,5]. Fillers are mainly naturally occurring minerals such as kaolinite, precipitated calcium carbonate (PCC), titanium dioxide, silica, and silicate [5-9]. Those minerals have colloidal characteristics with mean particle diameter sizes of less than 2 μm, and thus they form very stable suspensions which are difficult to settle and consolidate. Paper mill industries use high volume of fresh water (250-300 m^3) per metric ton of produced paper [10]. Due to strict worldwide environmental regulations, the effluent from these plants must be treated in an environmentally and economically acceptable manner. However, the poor operating procedures followed in industrial wastewater treatment may lead to overdesign, unnecessary cost and inefficiency in such effluent treatment operations. Extensive research is required to optimize the use of different polymers as flocculants to improve the dewatering process of such colloidal suspensions.

Flocculating these colloidal particles using electrolytes and polyelectrolytes into bigger flocs is a common procedure to provide an efficient separation [6]. The produced flocs have a typical range of sizes between a few microns to several hundred microns or even larger [11]. However, the type of the polyelectrolytes, molecular weight, surface charge density, flocculation conditions and solids particle fractions during the flocculation are important factors which can influence the size, structure and strength of the produced flocs [12-15]. Usually, floc properties, such as fractal dimension, density and settling velocity, are powerful parameters used in measuring the performance of the flocculation processes [16-19]. In addition to structure, floc strength is also an important parameter to describe floc properties [7-9,13,15,20-23]. Floc must be strong enough to resist the applied pressure/stresses during the sedimentation, and filtration [24]. Otherwise, the flocs will be destroyed to smaller particles, which will have lower removal efficiencies during the sedimentation and filtration processes. Therefore, there is a tremendous opportunity for optimization of such industrial wastewater treatment through manipulation of the parameters that influence the flocculation and rheology. Relating the degree of flocculation to the rheological characteristics of the flocculated colloidal, particles will have greater impact on overall treatment process.

To the best knowledge of the authors, only few researchers have studied flocculation of real industrial papermaking suspension effluents [10,22,25,26]. Also, only a few papers have studied the rheol-

†To whom correspondence should be addressed.
E-mail: m.nasser@qu.edu.qa

ogy of real industrial papermaking suspension [27,28]. But, all of the references mentioned above study either the flocculation of papermaking suspension or their rheological behavior without bearing in mind any relationships between them. Linking different types of experimental studies of such colloidal minerals is difficult, because even if the colloidal mineral has the same mineralogy it frequently comes from different sources and undergoes different usages prior to experiment. Evidently, it is easier to search for links if the same system is used.

In this study, fundamental studies were carried out on the use of different rheological methods to understand the behavior of real industrial papermaking suspension under different types of shear. The observed results were quantitatively related to the degree of flocculation for the same industrial papermaking suspensions reported in our previous paper [6]. In addition, adsorption measurements were also performed to validate the rheometric findings. Degree of flocculation parameters such as settling rate, floc size and effective floc density were linked to the adsorption and the rheological parameters such as Bingham yield stress, critical stress, creep compliance, elastic and viscous moduli. The results presented in this study can be used as strong tools to examine the compressibility and elasticity behavior of the flocculated networks, thereby, relating these properties to the mechanical limit of the material during the sedimentation and dewatering process.

THEORY

1. Bingham Yield Stress

Bingham yield stress model adopts a linear relationship between shear stress (τ) and shear rate (γ). The shear stress at intercept point is being distinct as Bingham yield. Bingham yield stress is defined as [29]:

$$\tau = \tau_B + \eta_B \gamma \tag{1}$$

where τ_B is the Bingham yield stress and η_B is the Bingham viscosity. The value of τ_B can be determined by extrapolating the linear part of the flow curve to zero shearing rate [30].

The magnitude of τ_B is a valuable parameter for the studying the strength of floc in a flocculated colloidal suspensions such as those existing during the pumping operations encountered during processing. Some authors [30,31] defined that τ_B is expressive of the amount of stress essential to decrease a flocculated suspension to a suspension containing only individual particles, i.e., the basic particles from which the floc is assembled [32].

2. Viscoelastic Properties

In oscillatory test, materials are subjected to deformation (in controlled rate instruments) or stress (in controlled stress instruments) which varies harmonically with time. This material deformation proceeds by applying an input strain ($\gamma = \gamma_o \sin(\omega t)$) and observing the following shear stress ($\tau = \tau_o \sin(\omega t = \delta)$). The γ_0 is the maximum amplitude of the strain and τ_0 is the maximum stress displaying the amplitude. The shear stress output from sinusoidal strain input can be defined as [33]:

$$\tau = \gamma^o (G' \sin\omega t + G'' \cos\omega t) \tag{2}$$

where G′ is the elastic modulus and G″ is the viscous modulus. The viscoelastic properties of the material are mainly defined in terms of elastic modulus (G′) and viscous modulus (G″). These parameters are dependent on strain or stress at low stress amplitude value. The linear region where the G′ and G″ were not strain or stress dependent is called the linear viscoelastic region (LVR). The critical stress (τ_c) is the stress matching the end of the extended linear viscoelastic region. During the oscillation, the arranged systems will receive energy from the oscillatory motion, and this energy is stored in the systems and is described as elastic modulus (G′), which is also called the storage modulus. On the other hand, oscillatory shear may also create irreversible deformations in a structured system, causing energy loss and the associated parameter is the viscous modulus (G″), which is also known as the loss modulus.

Starting with Eq. (2), the complex dynamic modulus (G*) can be obtained. G* is resolved into two component vectors, Elastic modulus (G′) and the viscous modulus (G″). The elastic properties of the solution are described by G′, and G″ is proportional to the viscous energy dissipated during flow. Eq. (3) relates the three moduli [29]:

$$G^* = G' + iG'' \tag{3}$$

While Eq. (4) defines the absolute value of the complex dynamic modulus (|G*|) [29].

$$|G^*| = \sqrt{(G'(\omega))^2 + (G''(\omega))^2} \tag{4}$$

Viscoelastic material also possesses complex dynamic viscosity (η^*) where:

$$\eta^* = \frac{G^*}{\omega} \tag{5}$$

In this equation ω denotes the angular frequency in rad/s.

Oscillatory rather than steady shear measurements were used to avoid any destruction of the networks of the flocculated suspension in the presence of PAM. Complex viscosity and elastic modulus are important measures for the system viscoelastic properties. Two of the oscillatory measurement modes were used to explore the viscoelastic properties of flocculated dispersions [29]:

2-1. LVR/Single Frequency Sweep

A strain or stress sweep, performed by changing the amplitude of the input signal at a constant frequency, was used to determine the limit of the LVR by identifying a critical value of the sweep parameter.

2-2. Frequency Sweep

In this test, the frequency was increased while the amplitude of the input signal (stress or strain) was fixed. To investigate the frequency sweep within the LVR, the value of the input signal (stress or strain) was kept lower than the critical value of stress or strain in the LVR of the measured samples.

3. Creep Test

In a creep test, a sudden stress (τ) is applied to the material and as a result the variation in strain (γ) which is known as creep is detected as a function of time. Creep parameter may be defined in terms of a creep compliance function (J). Eq. (6) defines the creep compliance function [29].

$$J = f(t) = \frac{\gamma}{\tau} \quad (6)$$

When the stress is removed, the material attempts a restore the original structure and shape. These tests are very important in identifying the material's behavior that exists in constant applied pressure/stress environments applications where gravity is the major driving force [34]. Compliance data are generated at different applied stress level and the measurements must be conducted within the range of LVR. Four element Burger model can be used to identify the creep compliance parameters [35,36]:

$$J = f(t) = J_o + J_1\left[1 - \exp\left(\frac{-t}{\lambda_{ret}}\right)\right] + \frac{t}{\eta_o} \quad (7)$$

where J_o is the instantaneous compliance, J_1 is the retarded compliance, η_o is the Newtonian viscosity of the free dashpot and λ_{ret} is the retardation time of the Kelvin component.

EXPERIMENTAL

1. Materials

The industrial papermaking suspension was received from Fletcher Limited, UK. The sample contains two types of fibers, namely softwood and hardwood fibers and participated calcium carbonate (PCC). The diameter of the softwood and hardwood fibers was 290 nm and 310 and respectively. Field emission SEM (FESEM) was used to measure the fiber diameters. Table 1 summarizes the composition of the papermaking suspension used in this study. The pH, turbidity (NTU) and zeta potential (mV) of the used PCC are 9.8, 208 and −23.7 respectively. The initial charge density of PCC used in the papermaking suspension is −1.3 meq/kg (the ionic charge of the slurry: −272 μeq/L). To achieve the desired fibrillation level, both softwood and hardwood fibers were sheared under very high pressure using microfluidizer of ten passes. All the suspensions were produced at around 4% (wt/wt). For floc size and rheological measurements, the mixture was mixed in distilled water and the required flocculant (polyacrylamides) was added; subsequently, the mixture was further mixed for 30 minutes using high speed mixer at 11,000 rpm and then aged for 24 h.

The anionic and cationic polyacrylamides (PAMs) based flocculant used in this study were provided by Cytec industries Inc., UK. Table 2 summarizes the characteristics of the three anionic and cationic PAMs. The average molecular weight of those PAMs was approximately 10-12 million Dalton. In addition, sulfuric acid (H_2SO_4) and sodium hydroxide (NaOH) were used for pH adjustment.

Table 1. Composition of papermaking suspension before the addition of flocculants

Component	Concentration (g/L)
Precipitated calcium carbonate	7.94
Hardwood	2.65
Softwood	2.19

Table 2. Type of the PAMs used in this study

PAM	Charge type	Percentage charge group on chain
C492	Cationic	10
C496	Cationic	35
A130LMW	Anionic	35

2. Methods

2-1. Polyelectrolytes Adsorption Experiments

For adsorption studies, experiments were carried out in 250 ml flasks by adding a known dose of flocculants to the papermaking suspensions. The suspension was stirred by a rotating shaker at 120 rpm for 24 hours. The flocs were centrifuged at high speed until all the residual colloidal particles were removed, the clear supernatant was transferred and then titrated with a solution of potassium polyvinylsulfate (KPVS), and toluidine blue dye was used as the indicator [37,38]. This technique was not effective for measuring the changes in anionic polyacrylamide concentration, so some modifications were adopted. The anionic PAM solution was treated first with solution of polydimethydiallylammonium chloride (PDMDAAC), which was then back titrated with KPVS by using the toluidine blue dye as indicator.

2-2. Rheological Measurements

In our previous paper, the optimum polyacrylamide doses were determined for the same industrial papermaking suspension used in this study [6]. The optimum doses were determined using different measurements, including settling rate, floc size, floc effective density, zeta potential, and turbidity measurements. In this paper, the rheological measurements were at room temperature using a controlled stress instrument (Bohlin C-VOR rheometer, Malvern Instruments, UK). In all tests, cup (26 mm diameter) and bob (25 mm diameter and 28.5 mm length) measuring geometry was used. Time sweep measurements were performed first to select the time before measurement needed to reach stable rheology (morphology). This equilibration time before measurement is usually used in each experiment as one of the entries before conducting the test. Equilibrium time of 5 minutes was given for the sample before applying any stress.

For τ_B measurement, the samples were sheared by increasing the applied shear stress from 10^{-2} to 1.0 Pa using a ramp time of 600 sec. Once the curve of shear stress as a function of shearing was plotted, τ_B was estimated by extrapolating the linear part of the flow curve to zero shearing rate. Results were reproducible and smooth flow-curves were consistently obtained, indicating that slip-stick effects were minor.

The values of G′, G″ and τ_c were determined as a function of applied stress in the range of 10^{-2}-10 Pa using a fixed frequency of 0.05 Hz. The values of G′ and G″ were measured by extrapolating the low stress plateau to zero and the critical stress is defined as the stress where elastic modulus falls to 90% of the plateau value. For the frequency sweep, a stress of amplitude 0.05 Pa, which is in the LVR for all the samples investigated herein, was applied, with frequencies between 0.01-0.5 Hz, and both G′ and G″ were measured as a function of the oscillation frequency. Amplitude of stress of 0.05 Pa is applied for the creep compliance as a function of time measurements. In this study all the experimental results were reproducible with error less than 5%.

Table 3. Floc sizes, settling rates and effective floc densities of papermaking suspensions flocculated using the optimum PAM concentration and at pH 9.8 (Nasser et al., 2013)

PAM	Floc size (cm)	Settling rate (cm s^{-1})	Floc effective density (g cm^{-3})
A130LMW	0.212	0.721	0.00629
C492	0.169	0.648	0.00889
C496	0.109	0.463	0.01528

RESULTS AND DISCUSSION

1. Optimum Flocculation

In a previous paper [6], we determined the optimum flocculant C492, C496 and anionic A130LMW polyacrylamides (PAM) dosages for papermaking suspension flocculation at pH 9.8 (the pH of real industrial papermaking suspensions). The optimum PAM concentration was defined as the concentration corresponding to maximum settling rate and minimum turbidity (or maximum supernatant clearance). Floc size and floc effective density measurements were also used as a tool for the optimum dose determination. It was found that the optimum concentration of A130LMW, C496 and C492 was within the range 0.5 to 1.0 mg/L. In this study, a 0.75 mg/L was used as the optimum dose for all the three PAMs. Table 3 summarizes the floc sizes, settling rates and effective floc densities of papermaking suspensions flocculated using the optimum PAM concentration at pH 9.8 [6].

2. Adsorption

Fig. 1 shows adsorption data for papermaking suspension as a function of PAM dose at pH 9.8. The adsorption of the anionic and cationic PAMs happens through hydrogen bonding between the solid surface and the polyacrylamide's primary amide functional groups [6].

In the case of cationic C492 and C496, the attraction forces between the positively charged PAM and the negatively charged PCC promote the adsorption mechanism and the amount of adsorbed increased with increasing the C492 and C496 concentrations. On the other hand, the adsorption behavior of cationic PAM on to PCC surface is dependent on the charge density of the PAM.

The results show that the adsorption rate increases with increasing the polyacrylamide surface charge density. The maximum PAM adsorbance of cationic C492, which has a charge density of 10%, was 0.82 mg g^{-1} PCC using 4 mg/L of C492. This value was increased to 1.29 mg g^{-1} PCC for the case of C496 using the same PAM concentration. This was anticipated here since the attractive forces between the positively charged PAMs chains and the negatively charged particle surface increase with increasing the surface charge density; thus the number of connection points between the C496 chain and PCC surface is higher than in the case of C492. The results also show the bridging is weakened as the adsorption rate increases, because the surface sites of the particles, which are vacant for bridging, are decreased. Therefore, bridging in C492 is much more effective than in C496 based PAM. This could be the reason why the flocs produced by 35% surface charge (i.e., C496) are smaller than the flocs formed by 10% surface charge (C492).

In the case of anionic A130LMW adsorption is still possible through hydrogen bonding between the solid surface and PAM's primary amide groups. However, due to the electrostatic repulsion between the negatively charged A130LMW and negatively charged PCC, surface will overcome the attractive van der Waals forces. These repulsive forces reduce the adsorption rate and the maximum adsorption value measured for A130LMW was 0.366 mg g^{-1} PCC using 4 mg/L of A130LMW, and this is considerably smaller compared with two cationic PAMs.

3. Flow Behavior

Fig. 2 shows shear stress as a function of shear rate for papermaking suspension flocculated using different PAMs at pH 9.8. τ_B was estimated by extrapolating the linear part of the flow curves to zero shearing rate. The values of τ_B were 0.210, 0.298 and 0.310 Pa for A130LMW, C492 and C496 respectively. This is expected here, since the electrostatic attractions between the positively charged cationic C492 and C496 PAM and the negatively charged PCC promote the adsorption (see Fig. 1) and produce strong and dense flocs (see Table 3). Subsequently, the stress required to break the flocs, τ_B, is higher as well. In the case of anionic A130LMW, the repulsion force between anionic PAM and solid surface lets the PAM molecules to be stretched and to yield loops and tails, which leads to the production of weak, larger and open-structured flocs of less dense than those produced when cationic polyacrylamides (see Table 3). Therefore, the stress essential to break the flocs, τ_B, is lower as well.

Fig. 3 shows hysteresis loops for papermaking suspension floc-

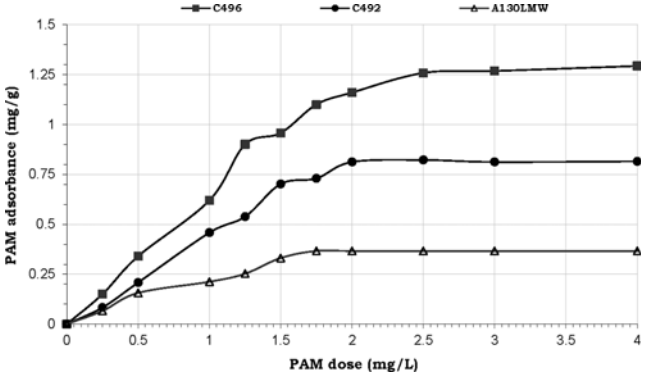

Fig. 1. Adsorption isotherms for papermaking suspension as a function of PAM dose at pH 9.8.

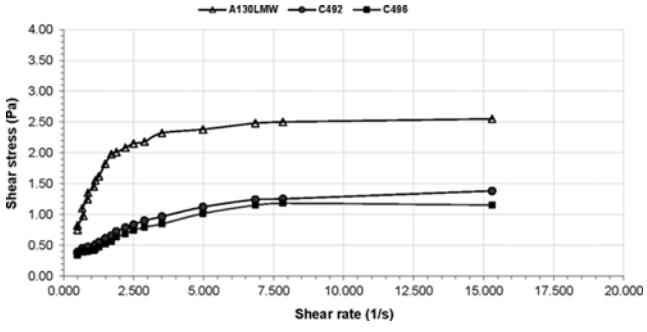

Fig. 2. Shear stress as a function of shear rate for papermaking suspension flocculated using different PAMs at pH 9.8.

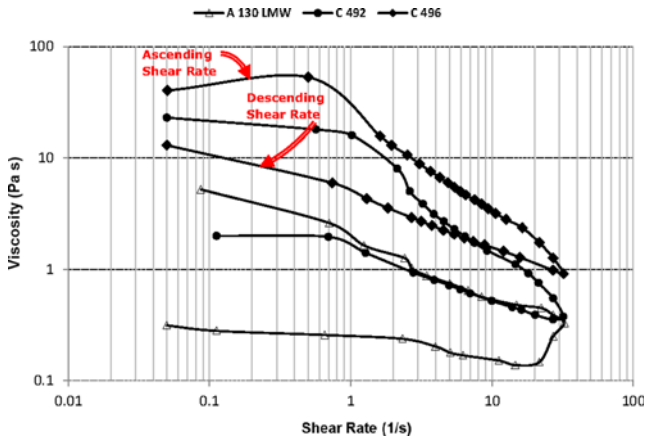

Fig. 3. Shear rate sweep tests for papermaking suspension flocculated using different PAMs at pH 9.8.

culated using different PAMs at pH 9.8. The measurements were carried out with ascending (forward measurements) and descending (backward measurements) shear rates for 250 s. The results revealed that the papermaking-PAM suspension used in this study had a non-Newtonian, shear thinning, thixotropic behavior. The presence of hysteresis loops (i.e. the area between the ascending and descending shear rates) was an indication of the shearing effect on the papermaking suspensions flocs. In other words, there is an irreversible, shear induction damaging the network of the flocs. The hysteresis loop area may be assumed to be the difference between the energies required for structural breakdown and rebuilding. It can be seen that the viscosity of the suspension decreased with increasing the shear rate. The gap between the ascending and descending viscosities was largest for the papermaking suspension flocculated using anionic PAM (i.e., A130LMW); however, the gap was reduced when papermaking suspension flocculated using cationic PAM. On the other hand, the time-dependent behavior of the papermaking suspension flocculated using different PAMs at pH 9.8 was investigated and the results are shown in Fig. 4. The samples were sheared at a constant shear rate of 25 s^{-1}. It is clear that the viscosity of the flocculated suspensions decreased with the shearing time

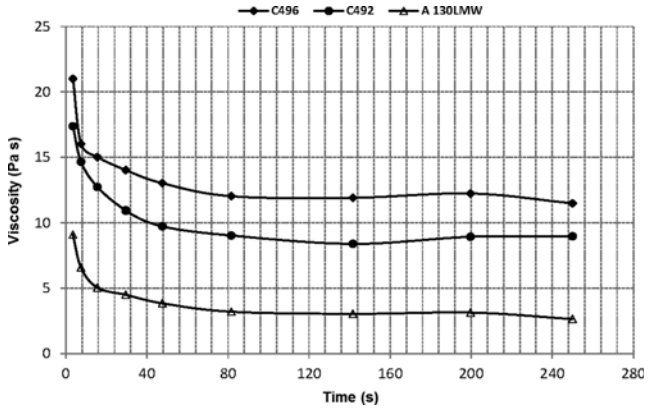

Fig. 4. Constant shear rate tests for papermaking suspension flocculated using different PAMs at pH 9.8.

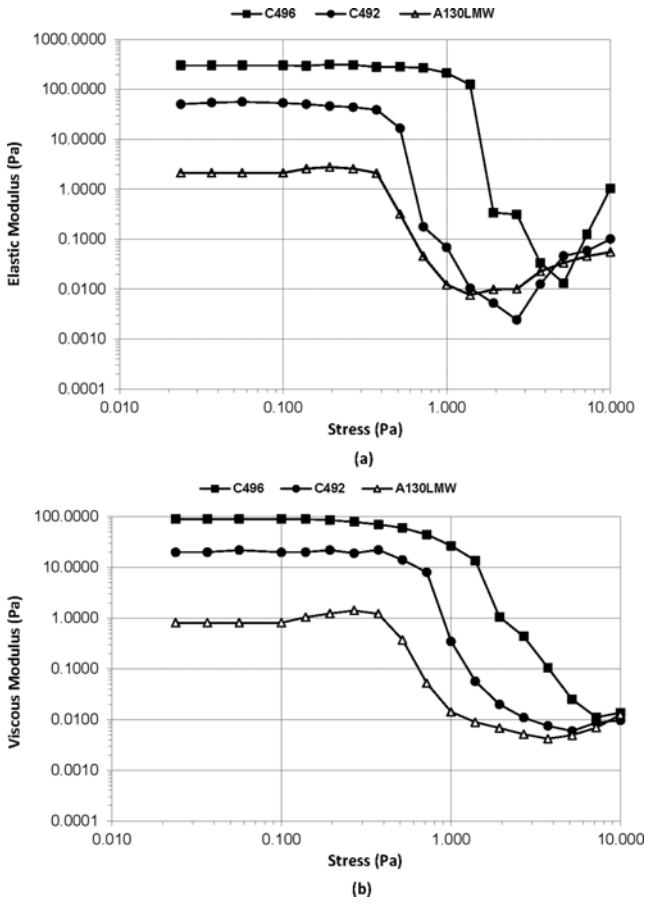

Fig. 5. Elastic and viscous moduli as a function of the applied stress for industrial papermaking suspension flocculated using PAM at pH 9.8. All data were obtained at frequency of 0.05 Hz.

to reach an equilibrium state within 80 s for all of the samples. Papermaking suspensions flocculated using cationic C492 and C496 demonstrated higher viscosities than the suspensions flocculated using anionic A130LMW. As mentioned before, this is due to the strong electrostatic attractions between the positively charged cationic C492 and C496 PAM and the negatively charged PCC.

4. Viscoelastic Properties

Fig. 5 shows the elastic modulus, G′, and viscous modulus, G″, (at oscillation frequency 0.05 Hz) as a function of the oscillatory stress for papermaking-PAM suspension at pH 9.8. The values G′ and G″ were constant for a wide range of the tested stress, suggesting the independence of elasticity on the applied stress. However, at a certain critical stress (τ_c) both G′ and G″ decreased rapidly reaching a minimum. The decrease in G′ and G″ can be attributed to a breakdown of the weak floc structures, and this is typical for viscoelastic materials due to the increase in solid-like behavior at low stress/frequencies [39]. The extracted values of the τ_c, G′ and G″ for papermaking-PAM suspensions are listed in Table 4. It can be seen that the critical yield stress (τ_c) values show similar trends to Bingham yield stress (τ_B) (see Fig. 2). Fig. 5 also shows that both cationic and anionic PAM produce flocculated suspensions with G′>G″. The differences being more obvious in the cationic PAM based suspensions because the network structure is expected to be

Table 4. Critical stress, elastic modulus and viscous modulus for flocculated papermaking suspensions at optimum PAM concentrations and at pH 9.8

PAM type	Critical yield stress $\times 10^3$/[Pa]	Elastic modulus $\times 10^3$/[Pa]	Viscous modulus $\times 10^3$/[Pa]
C 496	1000	301552	90172
C492	720	5033	50351
A130LMW	518	2116	809

stiffer and the suspension behaved like elastic solids more than viscous liquids. Furthermore, the elastic modulus decreases by almost an order of magnitude when using A130LMW instead of C496 (see Table 4). The magnitude of G′ and G″ is a function of the number of interactions points between the PAM chains and solid surface and the strength of those interaction forces. The large values observed in the G′, G″ and τ_c data by the cationic PAM are proposed as did as τ_B and floc effective density data, that the number of the interactions between the solid surface PAM chains and the strength of those interaction force is greater in the case of cationic polyacrylamide than the anionic polyacrylamide. The results also showed that the cationic C496, which has higher surface charge than C492, produces flocs having more elastic than the cationic C492, proposing differences in the floc structures, which are not obvious in the Bingham yield stress measurements.

The dynamic frequency sweep tests were conducted using an applied stress of 0.05 Pa. Fig. 6 shows the frequency dependencies of G′, G″ for flocculated papermaking-PAM suspensions. The elastic modulus is almost independent of oscillation frequency below ~0.1 Hz in a way comparable to that observed in single frequency sweep measurements. The flocculated suspension showed large Bingham yield stresses are mainly linked to the existence of strong and dense flocs which have large G′, G″ and η^* at the frequencies used herein. Fig. 7 shows the frequency dependencies of η^* for flocculated papermaking-PAM suspensions. The decrease in η^* with the increase in frequency could be attributed to the same previous reasons of breakdown in the flocs structures.

The observations regarding the critical yield stress, τ_c, elastic modulus, G′, complex viscosity, η^*, and Bingham yield stresses, τ_B, measurements are in agreement with those made regarding the other degree of flocculation parameters such as turbidity measurements, settling rate, floc size and effective floc density made in our previ-

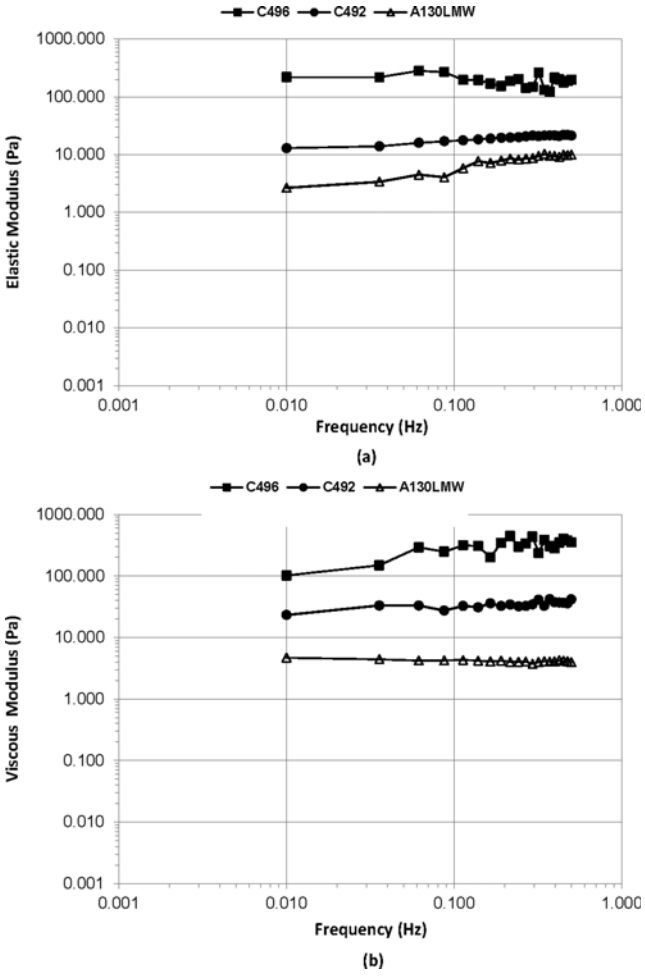

Fig. 6. Elastic and viscous moduli as a function of frequency for industrial papermaking suspension flocculated using PAM at pH 9.8. Amplitude of the applied stress is 0.05 Pa.

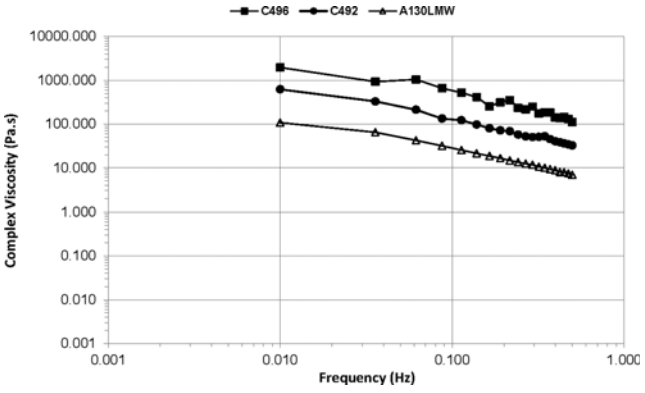

Fig. 7. Complex viscosity as a function of frequency for industrial papermaking suspension flocculated using PAM at pH 9.8. Amplitude of the applied stress is 0.05 Pa.

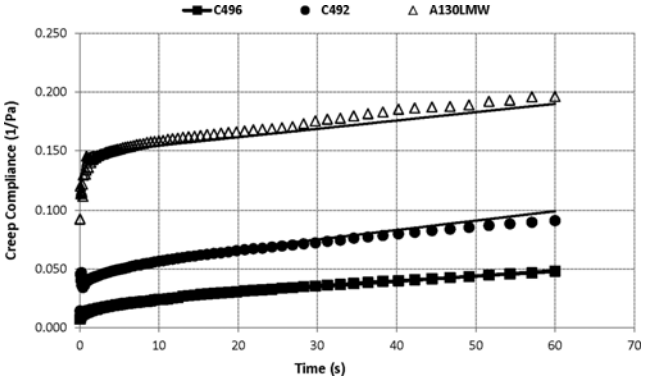

Fig. 8. Creep compliance as a function of time for industrial papermaking suspension flocculated using PAM at pH 9.8. Amplitude of the applied stress is 0.05 Pa.

Table 5. Fitting parameters of creep data using Eq. (5) for flocculated papermaking suspensions at optimum PAM concentrations and at pH 9.8

PAM type	$J_0 \times 10^3$ [1/Pa]	$J_1 \times 10^3$ [1/Pa]	λ_{ret} [s]	η_0 [Pa·s]
C 496	7.48	3.1	12.59	27778
C492	14.4	44.8	9.77	5000
A130LMW	94.2	83.5	7.75	3333

ous paper [6]. That is, highly flocculated dispersions with high settling rate, high effective density and low supernatant turbidity form strong flocs with significant G′, τ_c, η^*, τ_B and vice versa.

5. Creep Test

The experimental results for the creep compliance as a function of time for flocculated papermaking-PAM suspensions are shown in Fig. 8. It can be seen that the creep deformation is much larger for the anionic PAM based suspensions than for cationic PAM based suspensions. The continuous lines drawn in Fig. 8 is the four-element Burger model fitting using Eq. (6) and the fitting parameters are tabulated in Table 5.

J_o signifies the instantaneous floc deformation at time=0. The strong cationic PAM based suspensions showed lower J_o than the anionic PAM based suspensions. This proves that the flocs produced by cationic PAM based suspensions are mechanically stronger than those flocs produced by anionic PAM based suspensions.

η_o is used to identify the viscosity of the system, and the large values of η_o observed for the cationic PAM based suspensions again support the concept that the floc network structure produced by cationic PAM is stronger than those produced by anionic PAM. The results also showed that the effect of the applied stress of 0.2 Pa is insufficient to break all the structures of the flocs produced by cationic PAM and to force suspension to flow. However, the anionic PAM based suspensions showed less resistances to flow and these were clearly observed in the significant decrease in η_o and increase of J_1. The parameter J_1 is used as indication of the floc retardation deformation which is correlated to flocs structure breakdown.

The results also showed that the characteristic retardation time, λ_{ret}, is low for anionic PAM based suspensions. The large λ_{ret} means that the network structure of the flocs is strong, because flocculated suspensions with large retardation times reach full deformation slowly.

CONCLUSIONS

The effects of the surface charge type and density of polyacrylamides (PAMs) on the rheological behavior of real industrial papermaking suspensions were quantitatively related to the degree of flocculation for the same industrial papermaking suspensions. The results showed that the floc sizes were larger but less dense when anionic PAM was used, leading to the formation of open structure and loose flocs. However, the floc sizes were small but highly dense when cationic PAM was used, and this is due to the strong interaction forces between the positive cationic PAM and negative PCC surface. The rheological measurements performed in this study were in good agreement with the floc size and density measurements. The strong flocs produced by cationic PAM showed larger values of τ_B, G′, G″, τ_c and λ_{ret} than those produced by the anionic PAM. On the other hand, the results also revealed that increasing the cationic PAM surface charge density from 10% to 35% decreases the floc size but increases the adsorption rate, elasticity and effective floc density.

LIST OF SYMBOLS USED

τ : shear stress [Pa]
τ_B : bingham yield stress [Pa]
τ_0 : amplitude stress [Pa]
γ : shear rate [1/s]
η_B : bingham viscosity [Pa·s]
γ_o : amplitude strain
ω : frequency [Hz]
δ : phase angle
G′ : elastic modulus [Pa]
G" : viscous modulus [Pa]
G* : complex dynamic modulus [Pa]
τ_c : critical stress [Pa]
η : newtonian viscosity [Pa·s]
η^* : complex dynamic viscosity [Pa·s]
η_o : newtonian viscosity of the free dashpot [Pa·s]
J : creep compliance function [1/Pa]
J_o : instantaneous compliance [1/Pa]
J_1 : retarded compliance [1/Pa]
λ_{ret} : retardation time of the Kelvin component [s]

REFERENCES

1. J. Shen, Z. Song, X. Qian and F. Yang, *Carbohydr. Polym.*, **81**, 545 (2010).
2. C. Pan, J. S. Fu, S. J. Yuan and F. Long, *Chung-kuo Tsao Chih/China Pulp and Paper*, **31**, 30 (2012).
3. J. A. F. Gamelas, A. F. Lourenço, M. Xavier and P. J. Ferreira, *Chem. Eng. Res. Des.*, **92**(11), 2425 (2014).
4. R. J. Kerekes, *Nordic Pulp and Paper Research Journal*, **21**, 598 (2006).
5. M. S. Nasser, *Sep. Purif. Technol.*, **122**, 495 (2014).
6. M. S. Nasser, F. A. Twaiq and S. A. Onaizi, *Sep. Purif. Technol.*, **103**, 43 (2013).
7. S. Y. Lee and M. A. Hubbe, *Colloids Surf., A: Physicochem. Eng. Aspects*, **339**, 118 (2009).
8. M. R. Wu, J. Paris and T. G. M. van de Ven, *Colloids Surf., A: Physicochem. Eng. Aspects*, **303**, 211 (2007).
9. D. H. Yoon, J. W. Jang and I. W. Cheong, *Colloids Surf., A: Physicochem. Eng. Aspects*, **411**, 18 (2012).
10. M. A. A. Razali, Z. Ahmad, M. S. B. Ahmad and A. Ariffin, *Chem. Eng. J.*, **166**, 529 (2011).
11. M. S. Nasser and A. E. James, *Int. J. Miner. Process.*, **84**, 144 (2007).
12. L. Feng and Y. Adachi, *Colloids Surf., A: Physicochem. Eng. Aspects*, **454**, 128 (2014).
13. T. Li, Z. Zhu, D. Wang, C. Yao and H. Tang, *Int. J. Miner. Process.*, **82**, 23 (2007).
14. E. A. López-Maldonado, M. T. Oropeza-Guzman, J. L. Jurado-Baizaval and A. Ochoa-Terán, *J. Hazard. Mater.*, **279**, 1 (2014).

15. M. S. Nasser, F. A. Twaiq and S. A. Onaizi, *Miner. Eng.*, **30**, 67 (2012).
16. L. De Martín, J. Sánchez-Prieto, F. Hernández-Jiménez and J. R. Van Ommen, *J. Nanopart. Res.*, **16** (2014).
17. A. Vahedi and B. Gorczyca, *Water Res.*, **53**, 322 (2014).
18. J. Wu and C. He, *Int. J. Environ. Sci. Technol.*, **7**, 37 (2010).
19. A. Z. Zinchenko and R. H. Davis, *J. Fluid Mech.*, **742**, 577 (2014).
20. M. S. Nasser and F. A. Twaiq, *Chem. Eng. Res. Des.*, **89**, 768 (2011).
21. W. P. Cheng, P. H. Chen, R. F. Yu, Y. J. Hsieh and Y. W. Huang, *Int. J. Miner. Process.*, **100**, 142 (2011).
22. D. Wang, R. Wu, Y. Jiang and C. W. K. Chow, *Colloids Surf., A: Physicochem. Eng. Aspects*, **379**, 36 (2011).
23. W. Xu, B. Gao, Q. Yue and Q. Wang, *Sep. Purif. Technol.*, **78**, 83 (2011).
24. H. Chi, H. Li, W. Liu and H. Zhan, *Colloids Surf., A: Physicochem. Eng. Aspects*, **297**, 147 (2007).
25. A. Ariffin, M. A. A. Razali and Z. Ahmad, *Chem. Eng. J.*, **179**, 107 (2012).
26. R. J. Stephenson and S. J. B. Duff, *Water Res.*, **30**, 781 (1996).
27. W. K. J. Mosse, D. V. Boger and G. Garnier, *J. Rheol.*, **56**, 1517 (2012).
28. B. Derakhshandeh, R. J. Kerekes, S. G. Hatzikiriakos and C. P. J. Bennington, *Chem. Eng. Sci.*, **66**, 3460 (2011).
29. J. D. Ferry, *Viscoelastic Properties of Polymers*, John Wiley & Sons, New York (1980).
30. A. E. James and D. J. A. Williams, *Adv. Colloid Interface Sci.*, **17**, 219 (1982).
31. P. R. Williams, D. J. A. Williams and R. L. Williams, in "Theoretical and Applied Rheology", P. M. Keunings, Ed., pp. 949, Elsevier, Amsterdam (1992).
32. P. R. Williams, D. J. A. Williams and R. L. Williams, *Colloids Surf., A: Physicochem. Eng. Aspects*, **77**, 75 (1993).
33. D. V. Boger, *Exp. Therm. Fluid Sci.*, **12**, 234 (1996).
34. M. S. Nasser and A. E. James, *Colloids Surf., A: Physicochem. Eng. Aspects*, **317**, 211 (2008).
35. M. Balaban, A. R. Carrillo and J. L. Kokini, *Journal of Texture Studies*, **19**, 171 (1988).
36. M. Peleg, *J. Rheol.*, **24**, 451 (1980).
37. W. J. Chen, *Sep. Sci. Technol.*, **33**, 569 (1998).
38. M. S. Nasser and A. E. James, *Sep. Purif. Technol.*, **52**, 241 (2006).
39. W. Al-Sadat, M. S. Nasser, F. Chang, H. A. Nasr-El-Din and I. A. Hussein, *Journal of Petroleum Science and Engineering*, **122**, 458 (2014).